Design of Machines and Structures, Vol. 8, No. 2 (2018), pp. 52–58.
https://doi.org/10.32972/dms.2018.012

DESIGN ASPECTS OF A ROBOTIC END-EFFECTOR

LÁSZLÓ RÓNAI
University of Miskolc, Robert Bosch Department of Mechatronics
3515 Miskolc-Egyetemváros
ronai.laszlo@uni-miskolc.hu

Abstract: Design aspects of a robotic end-effector are discussed in this paper, which is planned to mount onto a Fanuc LRMate 200iC industrial robot. The end-effector is used for sophisticated assembling tasks therefore a load cell is built into the unit. It is a design target that the measured force in the gripper has only axial direction. The rest of the forces and torques are eliminated by two built-in thin plates. Strength analysis of the load cell and the stiffness effect of the plates are calculated and also considered in the assembling force values.

Keywords: *end-effector, FEM, load cell, strength analysis*

1. INTRODUCTION

Due to lack of human resources, nowadays even in Hungary more and more robots are applied in small and middle size companies. Robots are used not only for lading different workpieces but for sophisticated applications, e.g., assembling, welding, machining, etc.

The industry demands such robotics, which are based on haptic concept. The term haptic is originated from Greek, it means 'sense of touch' [1]. The machine haptic could be based on the one hand measurement of the forces, moments in the joints and on the other hand measurement by the end-effector. There is a great variety of commercially available end-effectors, which are used on robots. However special end-effectors often required in special purpose assembling tasks.

An elastic element with strain gauges, i.e., 6 axis force-torque sensor is developed in ref. [2] to create an intelligent end-effector for polishing operations. Naturally there are commercially available end-effectors equipped with force sensors [3] but those cannot be programmed, e.g., complicated industrial operations like snap-fit problems. However in ref. [3] also deals with the opportunity of the human hand guiding. Robotic grippers are also important in agricultural applications, e.g., for fruit harvesting [4].

3D printed fingertips can be useful in many fields like assembling. Ref. [5] contains three main types of 3D printed fingertips: integrated capacitive touch sensing, integrated bend sensors and integrated fingertips with electromechanical switches. Ref. [6] deals with a sensor fusion, which can perform robot force control. The device contains a 6 axis force sensor and an accelerometer.

The main purpose of this paper to design of an intelligent and relatively cheap end-effector, which equipped with a microcontroller (μC) and could be programmed

for sophisticated industrial assembling processes. The unit is planned to contain a load cell to measure the assembling force between ±200 N. Two plates are built in to constrain the deflection of the load cell only in one direction. Therefore the unit can measure the force only in axial direction.

The paper is organized as follows. In Section 2, the schematic of the planned end-effector is discussed. The strength analysis of the elements of the desired end-effector are detailed in Section 3. The FEM simulation of the load cell is performed by Autodesk Inventor 2016 software. The deflection-load curve of the two plates is also determined. The concluding remarks are presented in Section 4.

2. SCHEME OF THE END-EFFECTOR

In this section the design aspects of an end-effector are discussed. This unit consists of a load measurement system equipped with a μC and a traditional pneumatic gripper. The end-effector is planned to mount onto a Fanuc LRMate 200iC industrial robot. The mounting holes of the robot are shown in *Figure 1*, where the diameter of the light grey coloured connecting element is Ø 40 mm.

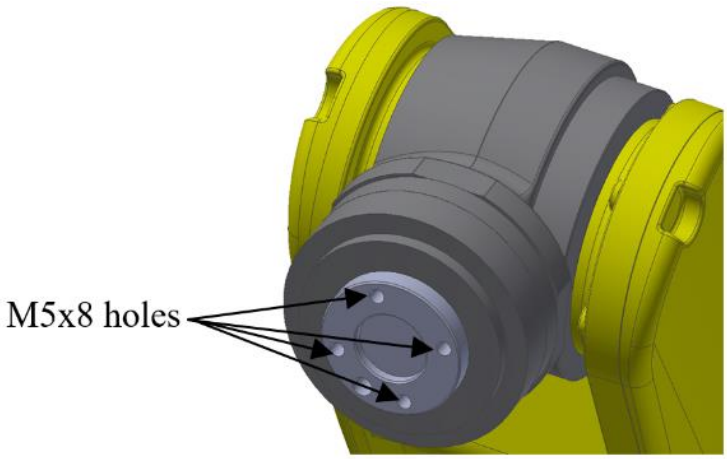


Figure 1. Connecting element of the robot with the mounting holes

The scheme of the end-effector is shown in *Figure 2*. The beam type load cell can measure the assembling force since it has four strain gauges, which are used in a Wheatstone bridge configuration. The load cell purposed to measure shear force in general. To perform accurate force measurement two steel rectangle plates are mounted onto the load cell, which is practically a flexible parallel mechanism. The ends of the plates are mounted onto the wall of the end-effector. Thus the structure will measure only the force in the direction of the assembly. A 24 bit sigma-delta A/D converter is built in the μC unit *(*see *Figure 2).*

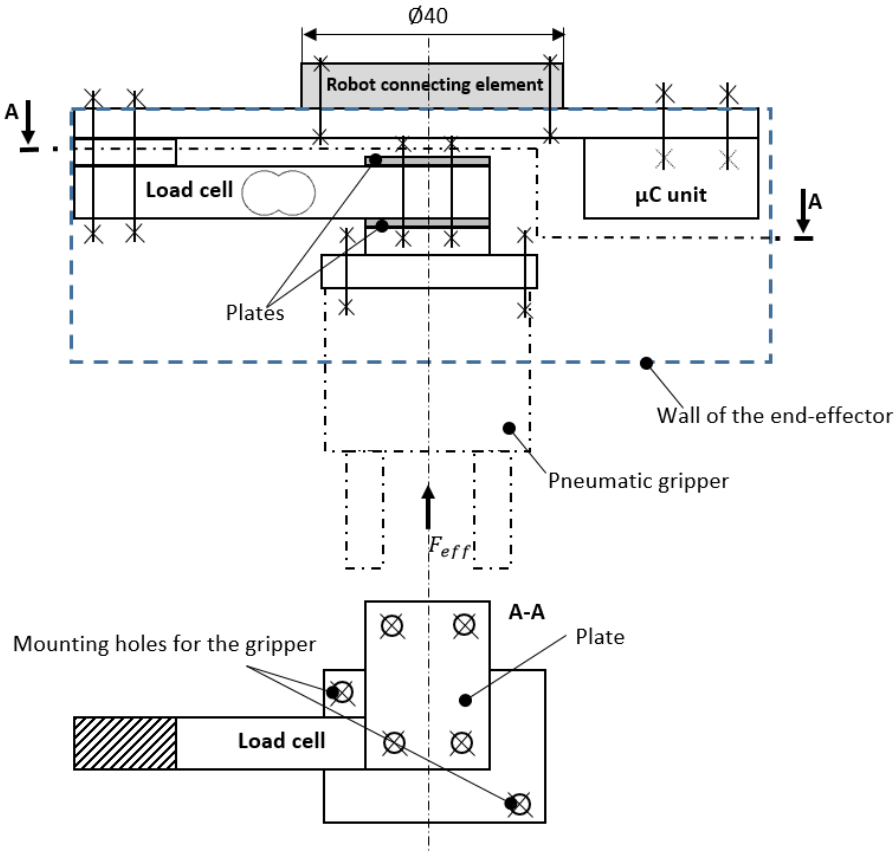


Figure 2. Schematic drawing of the designed end-effector

A Gimatic GS25 type pneumatic parallel gripper will be used to grip work pieces. It can be mounted onto the intelligent end-effector with two M6 × 12 threaded holes. One dowel pin and one centring disc are needed to set the reference position of the gripper. The robot has built-in pneumatic valves therefore the gripper will be actuated from the system program. The maximum closing force of the unit is 127 N at 6 bar pressure.

3. STRENGTH ANALYSIS OF THE STRUCTURAL ELEMENTS

It is worth to analyse numerically the load cell for the nominal load $F = 200\ N$ in order to determine the maximum deflection, which may occur also on the thin plates. It is assumed that both the load cell and the plates are linear elastic.

Finite element analysis has been performed by Inventor 2016 with a very fine mesh with number of nodal points 560,494 and number of elements 379,030. The displacement is constrained in two M5 holes where the load cell is fixed to the end-effector. The force $F = 200\ N$ is applied in the axis of the pneumatic gripper *(*see *Figure 2).*

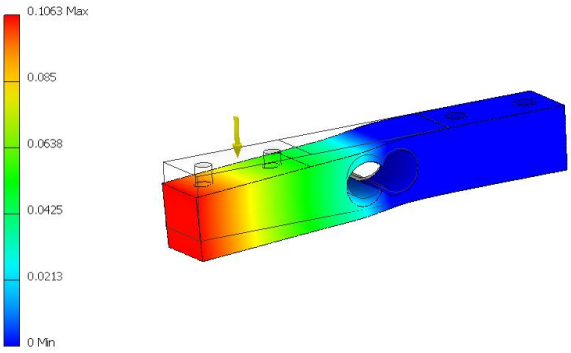


Figure 3. Deflection of the load cell

The deflection of the load cell is shown on *Figure 3* and the distribution of the strain ε_y is displayed on *Figure 4*. The maximum value of the displacement is $0.1063\ mm$. The strain distribution has got four local maximum values in the vicinity of the double cross holes where bending takes place. It should be mentioned that the strains of the opposite strain gauges are equal but with inverse signs. This fact allows the load cell to measure only shear force.

According to *Figure 2* rectangle thin plates are connected to the load cell and to the wall of the end-effector as well. One of the ends of the thin plate is clamped while at the other one the vertical displacement is free but the rotation is constrained as shown in *Figure 5*. In this case the plate is bended only in direction X.

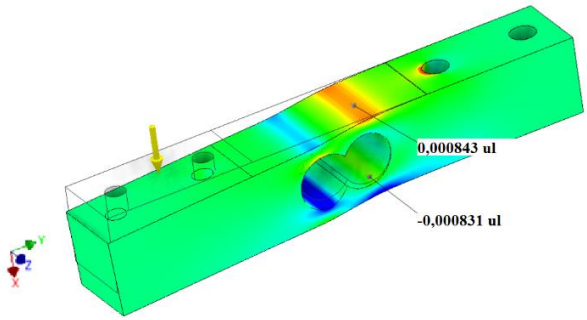


Figure 4. Strain ε_y of the load cell

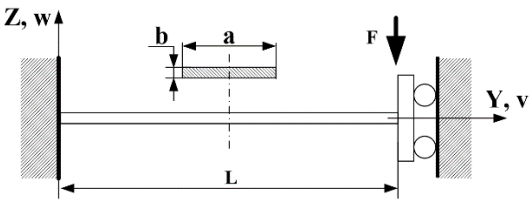


Figure 5. Bending model of the thin plate

This simple plate bending is analogues to a beam bending but it is a plain strain problem therefore the constitution parameters are different. For plate bending the elastic material parameter is calculated as:

$$E_1 = \frac{E}{1-\nu^2}, \tag{1}$$

where E is the Young's modulus, ν is the Poisson's ratio.

Table 1
Specification of the steel plates

	Value	**Dimension**
Thickness *(b)*	0.5	[mm]
Wideness *(a)*	23	[mm]
Length *(L)*	21	[mm]
Young's modulus *(E)*	210	[GPa]
Poisson's ratio *(ν)*	0.3	[–]

The model parameters of the thin plates, i.e., thickness b, width a, length L, Young's modulus E and Poisson's ratio ν are given in *Table 1*.

Since the plate is loaded and constrained only at both ends, thus one beam like finite element is enough to model the problem shown in *Figure 5*. Since there is an analogy between the beam and the single bending plate the stiffness matrix of one plate element can be written as [7], [8]:

$$\boldsymbol{K} = \begin{bmatrix} \frac{12IE_1}{L^3} & \frac{6IE_1}{L^2} & -\frac{12IE_1}{L^3} & \frac{6IE_1}{L^2} \\ \frac{6IE_1}{L^2} & \frac{4IE_1}{L} & -\frac{6IE_1}{L^2} & \frac{2IE_1}{L} \\ -\frac{12IE_1}{L^3} & -\frac{6IE_1}{L^2} & \frac{12IE_1}{L^3} & -\frac{6IE_1}{L^2} \\ \frac{6IE_1}{L^2} & \frac{2IE_1}{L} & -\frac{6IE_1}{L^2} & \frac{4IE_1}{L} \end{bmatrix}, \tag{2}$$

where L is the length of the plate and I is the area moment of inertia:

$$I = \frac{ab^3}{12}. \tag{3}$$

The equilibrium equation of the plate bending problem for one finite element is written as:

$$\boldsymbol{Kq} = \boldsymbol{f}, \tag{4}$$

where $\boldsymbol{f}$ is the column vector containing external force F, $\boldsymbol{q}$ is the vector of generalized nodal displacements

$$\boldsymbol{q^T} = [w_0 \quad \varphi_{x0} \quad w_L \quad \varphi_{xL}]. \tag{5}$$

The displacement boundary condition is given as

$$w(0) = 0, \varphi_x(0) = 0, \varphi_x(L) = 0, \tag{6}$$

it means that there is only one entry, i.e., displacement w_L, which is unknown. Therefore matrix equation (4) is simplified to the following scalar equation:

$$\frac{12IE_1}{L^3} w_L = F \tag{7}$$

Assuming that the displacement w_L is equal to the deflection of the load cell shown in *Figure 2* the supporting force of one plate is

$$F = \frac{12 \cdot 0.2396\, mm^4 \cdot 230769\, MPa}{9261\, mm^3} 0.1063\, mm = 7.6159N. \tag{8}$$

Since two parallel plates are connected to the load cell the effective load producing the maximum displacement will be increased twice of F given in (8), i.e., the force of the two plates is $F_p = 15.2318$ N.

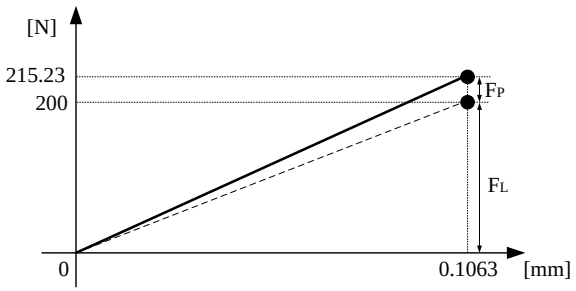


Figure 6. Original and the changed force displacement diagram

The effective load versus deflection diagram of the load measurement structure is shown in *Figure 6*, where the dashed line represents the force arising in the load cell F_L.

If the calibration is performed itself on the load cell then the strain gauges provides only the load cell force, which should be modified with proportional part of F_p in order to obtain the effective load at an arbitrary deflection w_L of the load cell:

$$F_{eff} = w_L \frac{F_L + F_P}{0.1063}. \tag{9}$$

4. SUMMARY

Design aspects of an intelligent end-effector has been discussed in this paper. A cheap beam type load cell, which measures the force has been built into the end-effector. Two thin plates have been connected to the load cell in order to constrain the undesired lateral deflection and axial rotations. This simple but advantageous constructional idea filters out those forces, which are acting not in axial direction.

Simple finite element plate model was used to determine the deflection force of the plates, which is necessary to involve to the determination of the effective axial force. The built-in μC makes it possible to program it for different characteristics of assembly forces, which enables it to handle specific tasks like snap-fit problems.

ACKNOWLEDGEMENT

The support of the ÚNKP-18-3 New National Excellence Program of the Ministry of Human Capacities is also acknowledged.

REFERENCES

[1] Srinivasan, M. A. (2005). *What is Haptics, The Touch Lab*. MIT.

[2] Ren, C., Gong, Y., Jia, F., Wang, X. (2016). Theoretical analysis of a six-axis force/torque sensor with overload protection for polishing robot. *23rd M2VIP International Conference, IEEE,* doi: 10.1109/M2VIP.2016.7827338, Nanjing, China.

[3] Loske, J., Biesenbach, R. (2014). Force-torque sensor integration in industrial robot control. *15th International Workshop on Research and Education in Mechatronics, IEEE,* doi: 10.1109/REM.2014.6920241, El Gouna, Egypt.

[4] Liu, J., Li, P., Li, Z. (2007). A Multi-Sensory End-Effector for Spherical Fruit Harvesting Robot. *International Conference on Automation and Logistics, IEEE,* doi: 10.1109/ICAL.2007.4338567, pp. 258–262, Jinan, China.

[5] Zapicu, A., Constantin, G. (2016). Additive Manufacturing Integration of Thermoplastic Conductive Materials in Intelligent Robotic End Effector Systems. *Proceedings in Manufacturing Systems*, Vol. 11, pp. 201–206.

[6] Grámez García, J., Robertsson, A., Gómez Ortega, J., Johansson, R. (2004). Sensor Fusion of Force and Acceleration for Robot Force Control. *Proceedings of International Conference on Intelligent Robots and Systems*.

[7] Páczelt, I. (1999). *Végeselem-módszer a mérnöki gyakorlatban*. I. kötet, Miskolc: Miskolci Egyetemi kiadó (in Hungarian).

[8] Bathe, K. J. (1996). *Finite Element Procedures*. Prentice Hall, Upper Saddle River, New Jersey.